

Role of lattice discreteness on brittle fracture: Atomistic simulations versus analytical models

Mariella Ippolito, Alessandro Mattoni, and Luciano Colombo*

Sardinian Laboratory for Computational Materials Science (SLACS, INFN-CNR)

and Department of Physics, University of Cagliari, Cittadella Universitaria, I-09042 Monserrato (Ca), Italy

Nicola Pugno

Department of Structural Engineering and Geotechnics, Politecnico di Torino, Torino, Italy

(Received 21 December 2005; published 20 March 2006)

By means of thorough atomistic simulations an energy-based theory, named quantized fracture mechanics, is commented and validated. This approach modifies continuum linear elastic fracture mechanics by introducing the hypothesis of discrete crack propagation, taking into account the discreteness of the crystal lattice. We investigate at an atomistic level the crack energy resistance for a matrix of silicon carbide with an isolated crack, and the effect on the stress at the crack tip due to a second phase particle. In both cases our results show that, while atomistic simulations provide the most basic level of understanding of mechanical behavior in nanostructured brittle materials, quantized fracture mechanics is able to effectively incorporate the main lattice-related feature, thus enlarging the realm of continuum modeling.

DOI: [10.1103/PhysRevB.73.104111](https://doi.org/10.1103/PhysRevB.73.104111)

PACS number(s): 62.25.+g, 62.20.Mk, 81.40.Np

I. INTRODUCTION

Modern materials technology is characterized by an ever-increasing rush toward miniaturization, e.g., in microelectromechanical (MEMS) and nanoelectromechanical (NEMS) systems, computer chips, bioengineering devices, and so on. Among several other issues an improved understanding of materials mechanical behavior at the nanoscale is indeed required. We might expect to find basic differences in solid mechanics at the macroscale (governed by continuum laws), or microscale (governed by dislocations, microstructural interfaces and microcracks), or nanoscale (governed by chemical bonding).¹ So, although solid mechanics is a well established field of investigation at the macroscopic level, a basic question is still open, whether continuum laws of mechanics are still valid at the nanoscale. In particular, this is the case of fracture mechanics that, on the one side it is initiated by a true atomistic-scale event like a bond snap, but on the other side does show up at the microscale, eventually driving to materials macroscopic failure. As a matter of fact, stress and strain fields computed by continuum theories at a vanishing distance from the crack tip become mathematically singular,^{2,3} thus making it hard to predict a relevant phenomena (like toughness or crack deflection) in the near vicinity of the crack tip.

The Griffith problem,²⁻⁴ describing a planar crack in an homogeneous medium, is a paradigmatic example to point out the limit of traditional linear elastic fracture mechanics (LEFM) in describing the mechanical response at the nanoscale. According to the Griffith theory, the total energy variation dU associated to a virtual increment of the crack dc (see Fig. 1) may be portioned into a mechanical dW and a surface dU_s term, so that $dU = dW + dU_s$. The crack propagates when the energy-release rate G , defined as $G = -dW/dA$, becomes larger than the intrinsic crack resistance, $G_C = dU_s/dA = 2\gamma_s$, necessary to create the new surface dA . Within LEFM, in a perfect homogeneous solid in vacuum, γ_s is identified with the unrelaxed cleavage surface energy γ .^{2,3,5} Such an identi-

fication $\gamma_s = \gamma$ is far from being generally valid in realistic systems and has motivated a large amount of numerical and analytical works in the past years.⁶⁻¹¹ As a matter of fact, it has been recently found⁹ that in realistic models for brittle solids γ_s turns out to be larger than γ which only provides a lower limit to crack resistance and, possibly, γ_s could be also direction-dependent.¹⁰ Furthermore, the cleavage surface energy is not a constant, rather it depends on the crack length and the state of deformation.

This example clearly proves that some critical re-addressing of the basic features of LEFM should be carried out in order to reconcile atomistics to continuum modeling. This is in fact the scope of the present paper. By means of an energy-based theory, named quantized fracture mechanics (QFM),¹¹ developed as a natural evolution of LEFM, we will discuss two case studies: The above isolated Griffith crack and a defect pair formed by a nearby crack and an elastic inclusion. While the first problem has a paradigmatic relevance, the second one is quite important for developing nano-composite materials, since the introduction of a second

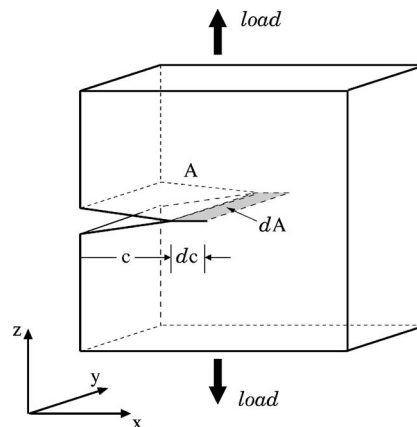


FIG. 1. Static plane-crack system, showing incremental extension of its length dc and surface dA .

phase fiber into a brittle material is an effective way to improve its fracture toughness.¹²

QFM theory is focused on the basic assumption that the medium is continuum, linear, and elastic everywhere. However, the hypothesis of discrete crack propagation is now introduced to take into account the underlying crystal structure. For vanishing crack length QFM predicts a finite ideal strength at the crack tip, and it has no restrictions on treating crack of arbitrary size and shape, in contrast to LEFM. Such a theory has been so far successfully compared with many experimental results on carbon nanotubes,¹³ β -SiC nanorods,¹⁴ and α -Si₃N₄ whiskers.¹⁵ The goal of the present work is to use atomistic simulations to further test the prediction of QFM, to firmly root such a theory into the atomistic picture, and to discriminate between QFM and LEFM.

We have focused our atomistic calculations on cubic silicon carbide (β -SiC) since it is the prototype of an ideally brittle material up to extreme values of strain and because of its technological relevance for structural and nuclear applications.¹⁶ Concerning the inclusions, we have considered the two cases of silicon (Si/SiC) and carbon (C/SiC) inclusions in SiC.

The paper is organized as follows. In Sec. II we introduce the basic concepts of QFM, in particular for the crack energy resistance in the Griffith geometry and the stress intensity factor at the tip of a crack facing a nanosized fiber. In Sec. III we describe the computational framework of present atomistic simulations, taking special care in describing the geometry. In Sec. IV we present our results and we extensively compare LEFM to QFM predictions.

II. QUANTIZED FRACTURE MECHANICS

According to Novozhilov,¹⁷ during the crack propagation there is a minimum crack extension (corresponding to the breaking of just one interatomic bond) that is named the *fracture quantum*. We like to stress that this somewhat unfortunate expression does not refer to any real quantum effect. Rather, it only underpins a discrete (versus continuum) formalism. We will adopt such a phrase for the sake of consistency with Refs. 11 and 17. Novozhilov proposed a modified fracture criterion based on stress, that at variance with LEFM takes into account the discreteness of the fracture event. In Mode I loading³ the critical stress is:

$$\sigma^{Nov} \equiv \frac{1}{a_0} \int_0^{a_0} \sigma_z(x) dx = \sigma_C, \quad (1)$$

where the load is applied along the z direction (see Fig. 1). In Eq. (1), $\sigma_z(x)$ represents the complete elastic stress field perpendicular to the xy crack plane in the near vicinity of the crack tip ($x=0$) and a_0 is the fracture quantum. The ideal strength of the material is σ_C . This criterion can only be used if the expression of the stress field is known everywhere. We note that this information is often quite hard to get.

At variance with the Novozhilov theory, QFM is based on an energy approach, still maintaining the hypothesis of discrete crack propagation. Moreover, the restriction identifying the fracture quantum with the atomic spacing is now re-

moved: More generally, the fracture quantum is the minimum length of crack advance, which could be larger than the atomic spacing.¹¹ It is important to note that QFM is complementary with respect to the Novozhilov approach so that Eq. (1) is still valid. In the QFM theory the usual Griffith criterion $G=G_C$ is modified by substituting differentials with finite differences:

$$G^{QFM} \equiv - \frac{\Delta W}{\Delta A} = G_C. \quad (2)$$

The corresponding condition for stability is $(\Delta G^{QFM}/\Delta A)_C < 0$. Moreover, the stress intensity factor (SIF), which is a measure for the singular stress term occurring near the crack tip,^{2,3} is now defined as

$$K_I^{QFM} \equiv \sqrt{\langle K_I^2 \rangle_A^{A+\Delta A}}, \quad (3)$$

where K_I^{QFM} and K_I are the SIF within QFM and LEFM, respectively, and the average is computed as $\langle f(x) \rangle_A^{A+\Delta A} = (1/\Delta A) \int_A^{A+\Delta A} f(x) dx$.

Consider first the case of a slit crack of length $2c$ in opening Mode I. The standard LEFM result for the failure strength is

$$\sigma_f^{LEFM} = \frac{K_{IC}}{\sqrt{\pi c}}, \quad (4)$$

where K_{IC} is the fracture toughness. On the contrary, according to QFM formulation, the failure strength depends on the fracture quantum a_0 :

$$\sigma_f^{QFM} = \frac{K_{IC}}{\sqrt{\pi(c + a_0/2)}}. \quad (5)$$

Notably, the difference with the LEFM case, no divergence is found for the vanishing crack length ($c \rightarrow 0$). This is the first important conceptual improvement: QFM removes any singularity from the formalism.

The ideal sharp crack, discussed above, can be regarded as the limit case of a blunt crack at vanishing tip curvature. The asymptotic LEFM stress field around the tip, for such a blunt crack, is¹⁸

$$\sigma(r) = \frac{K_I'}{\sqrt{2\pi r}} \left(1 + \frac{\rho}{2r} \right), \quad (6)$$

where ρ is the crack tip radius and K_I' is the corresponding fictitious SIF. As shown in Fig. 2, r is the distance from the center of the circular blunt notch; everywhere in the elastic medium $r > \rho/2$. By substituting Eq. (6) into Novozhilov equations, it is obtained the following condition for brittle crack propagation¹⁹

$$\int_{\rho/2}^{\rho/2+a_0} \sigma_z(x, \rho, K_I') dx = \sqrt{\frac{2a_0}{\pi}} \frac{K_I'}{\sqrt{1 + (\rho/2a_0)}} = \sigma_C. \quad (7)$$

For a slit ($\rho/a_0 \rightarrow 0$) Eq. (7) gives

$$\int_0^{a_0} \sigma_z(x, \rho=0, K_{IC}) dx = \sqrt{\frac{2a_0}{\pi}} K_{IC} = \sigma_C. \quad (8)$$

By comparing these two results it is found that:

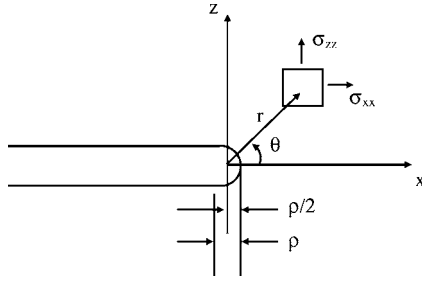


FIG. 2. Coordinates for the local stress distribution at distance r , ahead of a blunt crack of tip radius ρ .

$$K'_{IC} \approx K_{IC} \sqrt{1 + (\rho/2a_0)}. \quad (9)$$

K'_{IC} and K_{IC} are the fracture toughness for a blunt and a slit crack, respectively. According to Eq. (9) the blunt crack increases the toughness with respect to the case of the sharp crack. Once more, we point out that this result is notably different from a simplified correction to LEFM which predicts²⁰ $K'_{IC} \approx 2K_{IC}$ (i.e., no dependence upon the tip radius). The QFM failure stress for the blunt crack is obtained by replacing K'_{IC} , Eq. (9), in place of K_{IC} in Eq. (5)

$$\sigma_f^{QFM}(c, \rho) = K_{IC} \sqrt{\frac{1 + (\rho/2a_0)}{\pi(c + a_0/2)}} = \sigma_f^{LEFM} \sqrt{\frac{1 + \rho/2a_0}{1 + a_0/2c}}. \quad (10)$$

For the crack resistance energy we finally get

$$\frac{\gamma_s}{\gamma} = \frac{1 + \rho/2a_0}{1 + a_0/2c}. \quad (11)$$

At very short cracks (c of the order of few atomic spacings), γ_s/γ depends monotonically upon c . For the large crack ($a_0/c \rightarrow 0$) we get $\gamma_s/\gamma = 1 + \rho/2a_0 \geq 1$. We further remark that a_0 (which is related to the bond network) could also depend upon the direction of crack propagation. Accordingly, QFM can in principle account for the variation of the crack resistance with propagation direction, as indicated by some atomistic simulations.¹⁰

The QFM approach may be applied to the case of a crack interacting with an elastic inclusion, as well. According to the Eshelby theory,²¹ the variation of the SIF at the crack tip ΔK_{tip} , respect the case of the isolated crack (K_0), is $\Delta K_{tip}/K_0 = c_1/d^2$, where d is the crack inclusion distance and c_1 is a constant depending on the geometrical and elastic properties of the matrix and the inclusion. The QFM version of this law is obtained by using Eq. (3)

$$\begin{aligned} \frac{\Delta K_{tip}^{QFM}}{K_0} &= \sqrt{\frac{1}{a_0} \int_d^{d+a_0} \frac{\Delta K_{tip}^2}{K_0^2} dx} \\ &= \frac{c_1}{d^2} \sqrt{\frac{1 + a_0/d + 1/3(a_0/d)^2}{(1 + a_0/d)^3}}. \end{aligned} \quad (12)$$

In the limit of small a_0/d , this equation reproduces the same result predicted by the Novozhilov theory:

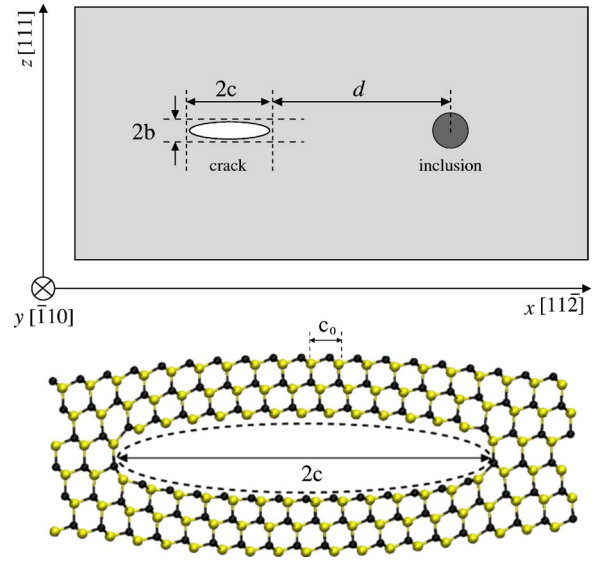


FIG. 3. (Color online) Top panel: Geometry and orientation of the simulation cell. For the case of an isolated crack the cell dimension L along x and z direction were the same ($22 \text{ nm} < L < 88 \text{ nm}$). For the case of crack-inclusion pair, x and z cell dimension were, respectively, 44.43 and 22.44 nm. In both cases the y dimension is 0.61 nm. Bottom panel: Atomic-scale view of the relaxed crack, where black (yellow) dots represent carbon (silicon) atoms.

$$\frac{\Delta K_{tip}^{nov}}{K_0} = \frac{1}{a_0} \int_d^{d+a_0} \frac{\Delta K_{tip}}{K_0} dx = \frac{c_1}{d^2(1 + a_0/d)}. \quad (13)$$

At very short crack-inclusion distances, $a_0/d \sim 1$, the QFM correction to the Eshelby theory is important.

III. ATOMISTIC SIMULATIONS

In order to reproduce at atomistic level the above geometries (i.e., the isolated crack and the crack-inclusion pair), we have considered a slab of perfect β -SiC monocrystal (see Fig. 3). The atoms interact through the bond-order Tersoff potential,²² well suited to study the mechanical properties of β -SiC.^{9,23,24} In particular such a force model is able to correctly reproduce the brittle failure of silicon carbide under tensile load once that a suitable modification of the potential has been operated according to Ref. 9. The stress fields were obtained by force relaxations based on the damped dynamics method. The convergence was controlled by monitoring the maximum atomic force and stress components, and the system was considered fully relaxed for atomic forces below 0.01 eV \AA^{-1} . The x , y , and z directions were aligned along the $[11\bar{2}]$, $[\bar{1}10]$, and $[111]$ orthogonal directions, respectively. In the x - y plane the system was kept fixed at the equilibrium lattice parameter of β -SiC (4.318 \AA) and periodically repeated. In the z direction the crystal was deformed by means of the constant traction method.²⁵ According to this method, periodic boundary conditions were removed along the z direction and the resulting surfaces [in our case one top silicon and one bottom carbon (111) shuffle planes] were subject to constant forces (tractions) to mimic the embedding

into an infinite bulk at the same condition of strain. This loading condition, corresponding to a fixed stress along z direction $\sigma_{zz}=\sigma_{zz}^{\infty}$ and fixed strain in the orthogonal plane $\epsilon_{xx}=\epsilon_{yy}=0$, represents the plane strain border condition of continuum mechanics.² The lowest unrelaxed surface energy of β -SiC is that of (111) shuffle plane, having the lowest density of dangling bonds. As a consequence, (111)-plane cracks is the most likely to form in experimental conditions, and therefore, we focused our theoretical analysis on such a crack arrangement. The crack was obtained by cutting the interatomic bonds across a segment of a central (111) plane in the deformed simulation cell.

For the case of an isolated crack we varied the crack length in the range $2c_0 < 2c < 50c_0$, where $c_0=2.644$ Å is the interbond distance along x direction (see Fig. 3, bottom panel). This choice resulted in a total number of atoms ranging from 3×10^4 up to 2.5×10^5 . Special care was taken in order to avoid finite-size effects: The imposed condition $L/c > 10$ corresponds to such a requirement. For any microcrack we varied the applied load up to obtain the critical condition of crack advance.

For the case study involving crack-inclusion interaction, a cylindrical fiber was introduced at some distance from the crack and centered on the same (111) plane (see Fig. 3, top panel). We have considered both a carbon and a silicon fiber, as prototype of tensile and compressive inclusion, respectively. The carbon and silicon fibers were created replacing silicon (carbon) atoms inside a cylindrical region by carbons (silicon) atoms. The actual fiber radius was 1 nm. As a result, coherent inclusions were obtained. In this case we used a fixed number of atoms (60 480) and the crack length was kept $2c=3.6$ nm. The applied load was varied so as to produce a resulting 3%–8% strain condition. We calculated the relative variation of the SIF at the crack tip by comparing the stress of a crack facing an inclusion, $\sigma_{CI}(x)$, with that of an isolated crack $\sigma_C(x)$ according to the following relation:

$$\frac{\Delta K_{tip}}{K_0} = \lim_{\delta \rightarrow 0} \frac{\sigma_{CI}(x_C + \delta) - \sigma_C(x_C + \delta)}{\sigma_C(x_C + \delta)}, \quad (14)$$

where δ is a vanishing distance from the crack tip.

IV. RESULTS: ATOMISTICS VERSUS QFM

A. Isolated crack

In order to compare atomistic simulations to QFM predictions for the isolated crack we calculated the failure strength at different crack-length values; the corresponding atomistic results for the crack resistance energy is reported in Fig. 4.

Within the LEFM theory (dot-dashed line in Fig. 4) the ratio γ_s/γ does not depend upon crack length. This is not the case of the atomistic data that increase up to a value $\sim 1.25\gamma$ at very long cracks. Part of this discrepancy was explained in a previous work⁹ by introducing the strain dependence of the surface energy and the Young modulus into the original Griffith formula for a sharp crack. It was found that the elastic theory for a sharp crack is not able to reproduce the atomistic results and the use of an elastoplastic model was proposed.

QFM results for a blunt crack suggest an alternative explanation of the atomistic data in terms of an intrinsic curva-

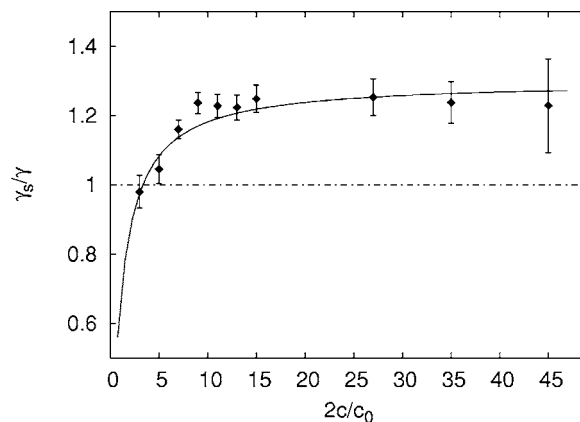


FIG. 4. Crack resistance γ_s as a function of the crack length $2c$ (unit of interbond distance c_0). The symbols are atomistic data; the dot-dashed line is the original Griffith theory; the full line is the fit of the atomistic data by QFM theory obtained for $a_0=0.25$ nm.

ture at the crack tip due to the lattice. According to QFM, it is found [Eq. (11)] that the crack-resistance energy of a blunt crack is higher than the sharp case and depends upon its length c . By approximating the atomistic crack with an elliptical hole (see Fig. 3), a rough estimation of the crack tip radius is $\rho=b^2/c$, where c and b are the major and minor axis of the ellipse, respectively. The radius turns out to be about one half of the interbond spacing $\rho \approx 0.45c_0$.

A fit of the atomistic data based on QFM result for blunt crack is represented in Fig. 4 as a full line. The fitted fracture quantum corresponds approximately to the interbond spacing, $a_0 \approx 0.94c_0$. The radius of curvature turns out to be $\rho \approx 0.55c_0$, which is consistent with the previous analysis. The QFM theory is nicely in agreement with the atomistic data and reproduces an increasing crack energy resistance for increasing crack length up to the asymptotic value $\gamma_s/\gamma \approx 1 + \rho/2a_0$ for infinite cracks. Notably the QFM result works well at very short crack lengths. Finally, we observe that the crack resistance predicted by traditional LEFM for a blunt crack does not depend upon the crack length and, therefore, atomistic data cannot be reproduced even considering a blunt crack. Accordingly, QFM represents an important improvement with respect to the LFEM theory for the isolated crack.

B. Interaction between a microcrack and an inclusion

The relative variation of the SIF at the crack tip was evaluated by using Eq. (14) at different crack-inclusion distances d and for both silicon a carbon inclusions. In the C/SiC case, the results are reported in Fig. 5. The intensification of the stress at the crack tip is reduced by the presence of the inclusion: Such a reduction is larger as the crack-inclusion distance decreases. The available LEFM continuum models predict this behavior only qualitatively.²³ In particular it has been proved²³ that the Li and Chen model,²⁶ based on the Eshelby theory,²¹ works well at large distances, while the Helsing model²⁷ is able to describe the stress intensification only at very short crack inclusion distances. In both cases, the best agreement with the atomistic data was

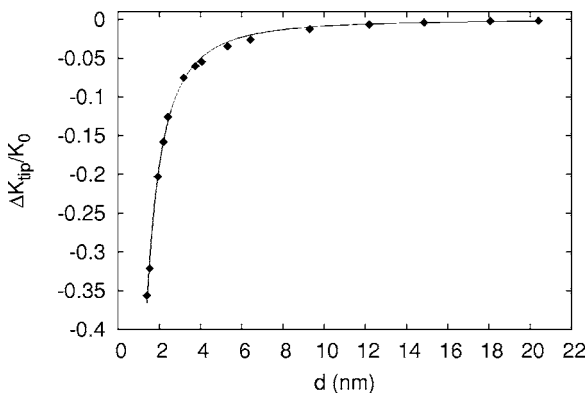


FIG. 5. Relative variation of the stress intensity factor at the crack tip, for β -SiC containing a diamond inclusion, as a function of the crack-inclusion distance d . The symbols are atomistic data and the full line is their best fit by QFM theory, $a_0=0.37$ nm.

obtained assuming for the inclusion radius a value larger than the effective one.

As in the case of the isolated crack, the QFM theory better reproduces atomistic data than LEFM models. The QFM fit of the atomistic results, obtained by using Eq. (13), is reported in Fig. 5 as a continuum line. Both a_0 and c_1 were used as adjustable parameters. The resulting fracture quantum is about the interbond spacing $a_0 \approx 1.4 c_0$ and $c_1 = -0.90$ nm². The agreement is good in the overall range of distances considered. We point out that by using the exact QFM relation, given by Eq. (12), in place of the approximated form provided by Eq. (13), the results are practically unchanged.

A similar analysis was carried out for the Si/SiC system as well. At difference with the carbon case the intensification of the stress at the crack tip is increased by the presence of the inclusion. The QFM best fit is reported in Fig. 6 as a continuum line. The fitted values are $a_0 = 5.36$ nm and $c_1 = 5.19$ nm². In this case the calculated fracture quantum is about 20 times larger than the interbond spacing. Conversely, if we set a_0 equal to the interbond spacing c_0 the agreement

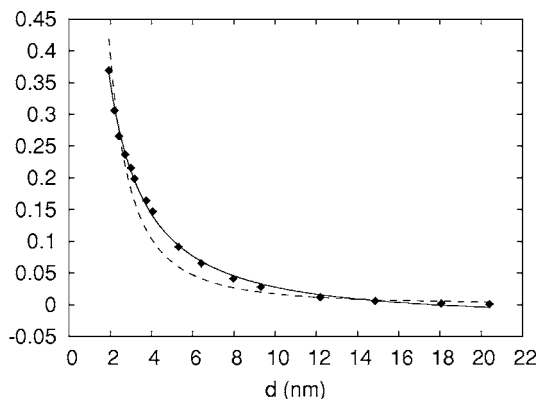


FIG. 6. Relative variation of the stress intensity factor at the crack tip, for β -SiC containing a silicon inclusion, as a function of the crack-inclusion distance d . The symbols are atomistic data and the full line is the QFM best fit, $a_0=5.36$ nm. The dashed line is the QFM fit corresponding to the choice $a_0=c_0$.

between atomistic and QFM theory (dashed line in Fig. 6) is not overall satisfactory. This result proves that the Novozhilov hypothesis¹⁷ (namely, the equivalence between the fracture quantum and the interatomic distance) has to be released in order to reconcile with the atomistic data. Present results clearly indicate that the quantum of fracture rather represents a measure of the length scale at which the QFM deviates from LEFM ($c_0 \rightarrow 0$). It turns out that such a length scale is much larger in the silicon than in the carbon case.

In order to understand the physical origin of the difference between the Si and C fibers, we studied the local nonlinear effect in the crack-inclusion interaction. As a matter of fact, it has been demonstrated²⁴ that the effect of the inclusion on the stress intensification at the crack tip falls beyond the linear regime. It is possible to define the *defect of linearity*²⁴ as the difference between the total stress of the system containing both the microcrack and the inclusion with that one calculated in a system containing just one crack or just one inclusion:

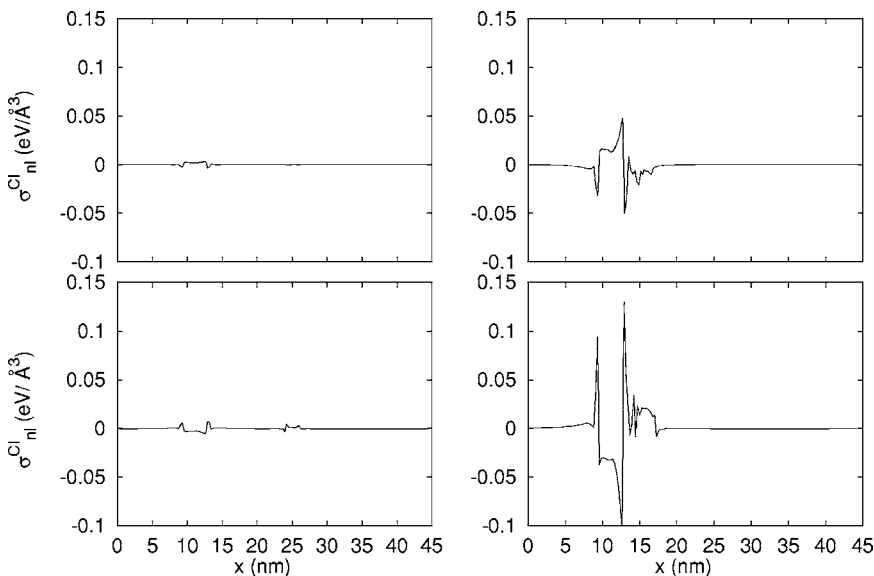


FIG. 7. Top panel: Defect of linearity $\sigma_{nl}^{Cl}(x)$ profiles for carbon inclusion, corresponding to crack inclusion distance $d=12.19$ nm (left) and $d=2.73$ nm (right). Bottom panel: Defect of linearity profiles for silicon inclusion, respectively, for $d=12.19$ nm and $d=2.73$ nm.

$$\sigma_{nl}^{CI}(x) = [\sigma_{zz}^{CI}(x) - \sigma_{zz}^{\infty}] - [\sigma_{zz}^C(x) - \sigma_{zz}^{\infty}] - [\sigma_{zz}^I(x) - \sigma_{zz}^{\infty}] \quad (15)$$

where the uniform stress background σ_{zz}^{∞} is subtracted to each term. According to Eq. (15), $\sigma_{nl}^{CI}(x)$ should vanish whether the interaction of the two defects is purely additive. Furthermore, $\sigma_{nl}^{CI}(x)$ depends on the relative distance between the two defects and in particular it increases as the crack inclusion distance decreases.

In Fig. 7 is reported the defect of linearity for the silicon (bottom) and carbon (top) inclusion cases. At large distances $\sigma_{nl}^{CI}(x)$ is vanishingly small for both. At difference, at distances $d \lesssim 6$ nm the $\sigma_{nl}^{CI}(x)$ for the silicon inclusion is larger than the carbon case by an amount of about $0.15 \text{ eV}/\text{\AA}^3$. This different behavior depends on the fact that the interatomic forces are not symmetric for bonds in high tensile or compressive state. As a matter of fact, the deviation from an ideal elastic model is larger in compression (Si/SiC) than in tension (C/SiC). Furthermore the Si/SiC lattice mismatch ($\approx 25\%$) is larger than the C/SiC mismatch ($\approx 18\%$). As a consequence, the silicon inclusion induces an higher local nonlinearity possibly responsible for the the very large fracture quantum.

V. CONCLUSIONS

The results of atomistic simulations have been compared with the predictions of the QFM theory in two different

cases. As far as concerns for the isolated crack, we have shown that the QFM theory explains the discrepancy between the atomistic crack energy resistance with respect to the LEFM case by means of two parameters: An intrinsic tip curvature and a fracture quantum. QFM agrees well with the atomistic data over all the investigated range of crack length, also providing a valuable estimation of the curvature radius. The quantum fracture for the isolated crack turns out to be close to the interbond spacing along the crack opening direction. As far as concerns for the crack-inclusion problem, we have studied the crack tip stress intensification for two kinds of nano-inclusions. QFM nicely reproduces the observed toughening and weakening effect induced by the carbon and silicon fiber, respectively. The quantum of fracture is a measure of the QFM correction to the LEFM and is much larger in the silicon case (about 20). We propose an explanation of this discrepancy in terms of the strong nonlinearity in the mechanical response observed for the Si/SiC system.

ACKNOWLEDGMENTS

We warmly acknowledge useful discussions with Alberto Carpinteri (Department of Structural Engineering and Geotechnics, Politecnico di Torino, Torino, Italy) and Fabrizio Cleri (ENEA Research Center, Roma, Italy). This work has been funded by MIUR under projects ‘‘PROMOMAT’’ and PON-‘‘CyberSar.’’ We also acknowledge computational support by CASPUR (Rome, Italy) computing center.

*Corresponding author. Electronic address: luciano.colombo@dsf.unica.it

¹B. R. Lawn, *J. Mater. Res.* **19**, 22 (2004).

²K. B. Broberg, *Cracks and Fracture* (Academic, San Diego, 1999).

³B. R. Lawn, *Fracture of brittle solids* (Cambridge University Press, Cambridge, 1975).

⁴A. A. Griffith, *Philos. Trans. R. Soc. London, Ser. A* **221**, 163 (1920).

⁵J. B. Rice, *J. Mech. Phys. Solids* **40**, 239 (1989).

⁶R. Thomson, C. Hsieh, and V. Rana, *J. Appl. Phys.* **42**, 3154 (1971).

⁷N. Bernstein and D. W. Hess, *Phys. Rev. Lett.* **91**, 025501 (2003).

⁸T. Zhu, J. Li, and S. Yip, *Phys. Rev. Lett.* **93**, 205504 (2004).

⁹A. Mattoni, L. Colombo, and F. Cleri, *Phys. Rev. Lett.* **95**, 115501 (2005).

¹⁰R. Perez and P. Gumbsch, *Phys. Rev. Lett.* **84**, 5347 (2000).

¹¹N. M. Pugno and R. S. Ruoff, *Philos. Mag.* **84**, 2829 (2004).

¹²J. D. Kuntz, G. Zhan, and A. K. Mukherjee, *MRS Bull.* **29**, 22 (2004), and references therein.

¹³M. F. Yu, O. Lourie, M. J. Dyer, K. Moloni, T. F. Kelly, and R. S.

Ruoff, *Science* **287**, 637 (2000).

¹⁴E. W. Wong, S. P. Xiao, P. E. Sheehan, and C. M. Lieber, *Science* **277**, 1971 (1997).

¹⁵H. Iwanga and C. Kawai, *J. Am. Chem. Soc.* **81**, 773 (1998).

¹⁶M. A. Capano and R. J. Trew, *MRS Bull.* **22**, 19 (1997).

¹⁷V. Novozhilov, *Prikl. Mat. Mekh.* **33**, 212 (1969).

¹⁸M. Creager and P. C. Paris, *Int. J. Fract. Mech.* **3**, 247 (1967).

¹⁹N. M. Pugno, B. Peng, and H. D. Espinosa, *Int. J. Solids Struct.* **42**, 647 (2005).

²⁰M. Drory, R. H. Dauskardt, A. Kant, and R. O. Ritchie, *J. Appl. Phys.* **78**, 3083 (1995).

²¹J. D. Eshelby, *Proc. R. Soc. London, Ser. A* **241**, 376 (1957).

²²J. Tersoff, *Phys. Rev. B* **39**, 5566 (1989).

²³M. Ippolito, A. Mattoni, L. Colombo, and F. Cleri, *Appl. Phys. Lett.* **87**, 141912 (2005).

²⁴A. Mattoni, L. Colombo, and F. Cleri, *Phys. Rev. B* **70**, 094108 (2004).

²⁵F. Cleri, *Phys. Rev. B* **65**, 014107 (2002).

²⁶Z. Li and Chen, *Eng. Fract. Mech.* **70**, 581 (2003).

²⁷J. Helsing, *Eng. Fract. Mech.* **64**, 245 (1999).